LANGMUIR

pubs.acs.org/Langmuir Article

Encapsulation of Graphene in the Hydrophobic Core of a Lipid Bilayer

Hadi Arjmandi-Tash,[‖] Lia M. C. Lima,[‖] Liubov A. Belyaeva, Tetiana Mukhina, Giovanna Fragneto, Alexander Kros, Thierry Charitat, and Grégory F. Schneider*

Cite This: *Langmuir* 2020, 36, 14478−14482 Read Online

ACCESS | Metrics & More | Article Recommendations | Supporting Information

ABSTRACT: Theoretical simulations have predicted that a lipid bilayer forms a stable superstructure when a sheet of graphene is inserted in its hydrophobic core. We experimentally produced for the first time a lipid−graphene−lipid assembly by combining the Langmuir−Blodgett and the Langmuir−Schaefer methods. Graphene is sandwiched and remains flat within the hydrophobic core of the lipid bilayer. Using infrared spectroscopy, ellipsometry, and neutron reflectometry, we characterized the superstructure at every fabrication step. The hybrid superstructure is mechanically stable and graphene does not disturb the natural lipid bilayer structure.

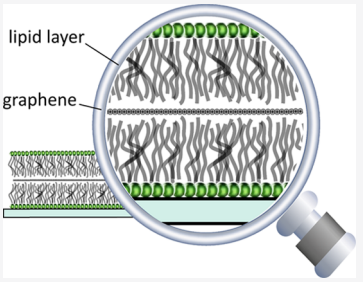

The growing interest in the application of two-dimensional (2D) materials in biorelated fields, e.g., biosensing,[1,2] medical diagnostics,[3] medical treatments,[4] bioimaging,[5] and drug delivery[6] motivates studying the biocompatibility of those materials. Particularly, examining the interaction of graphene-family materials with the lipid bilayer, as the simplified and standard model of a biomembrane, develops as an outstanding research line with the eventual goal of simulating more complex biological systems.[4]

Lipid bilayers are stable thermodynamic structures obtained from the self-assembly of amphiphilic lipid molecules.[7] Flakes of 2D materials, however, are thin enough to diffuse through the packed lipid molecules exhibiting dynamics, which could potentially perturb the integrity and order of the bilayer structure.[8] The lateral size, thickness, and oxidation degree of the flake, as well as its relative orientation with respect to the bilayer, govern the degree of damage.[9] Cryoelectron microscopy combined with the dye-leakage test demonstrated that the diffusion of large graphene oxide nanosheets would result in the splitting or even collapsing of a liposome.[10,11] Similarly, the sharp edges of a (reduced-) graphene oxide nanosheet can effectively rupture the bilayer by pulling out several lipids.[12] The strong interaction opens the transmembrane translocation pathway where water molecules leak from one side to the other,[13] which drives the antibacterial activity of (reduced-) graphene oxide.[14,15] Heterogeneous oxidation zones play a central role in transmembrane pathway formation.[10] The spontaneous lipid extraction is expected in boron nitride nanoflakes as well.[16] The phenomenon is different from those of thicker 2D materials, e.g., MoS_2: here, the disruption of the membrane is initiated by forming a dent upon collision with the flake, as opposed to the direct diffusion of the flake into the membrane.[17]

Pristine graphene, on the other hand, shows minimum destructive interaction:[10,13,18−20] small flakes (sizes comparable to the lipid molecule length) initially adsorb and remain flat on to the bilayer but gradually and partially penetrate into the structure as a result of the hydrophobic interaction between the nanoflake and the lipid tails.[13] In fact, engineering the hydrophobicity of graphene, e.g., by a customized coating of the nanoflake with single-stranded DNA is a potential approach to control the penetration depth of the nanoflake.[21] Partially inserted nanoflakes, however, is risky as it is prone to extract lipids from the bilayer to shield the protruding part exposed to water.[12]

Lipid dip-pen nanolithography, where a lipid-based ink is accurately delivered (written) on a graphene surface, has turned to be the standard method to realize lipid membranes on graphene support.[22−25] In fact, the hydrophobic interaction between graphene and lipid tails provides improved affinity of the lipids on graphene (e.g., compared to silicon dioxide substrate). The lipid solution spreads and covers the graphene surface uniformly. The bilayer lipid structure, however, is inverted in which the head groups of the lipids layers are in contact. The morphology of the graphene and also the polarity of the surface affects the compactness and the order of the lipids; particularly, simulations demonstrated a degraded order of the lipid bilayer on graphene compared to the free-standing

Received: June 8, 2020
Revised: October 15, 2020
Published: November 24, 2020

https://dx.doi.org/10.1021/acs.langmuir.0c01691
Langmuir 2020, 36, 14478−14482

bilayer.[25] Our group, however, developed an alternative approach for the fabrication of larger-area (centimeter scale) lipid−graphene heterostructures by the separate transfer of lipid and graphene monolayers, respectively, via the Langmuir−Blodgett and "top-fishing" approaches.[26] Particularly, we observed that covering the hydrophobic tail of a lipid monolayer with graphene improves the packing order. Here, we further develop that study by realizing a biomimetic hybrid system in which centimeter-scale graphene is sandwiched between two lipid monolayers. Large graphene sheets can be accommodated and remain flat between the hydrophobic lipid tails within the bilayer structure with negligible membrane disruption or lipid extraction. Such a structure is achieved by transferring a second lipid monolayer on top of the lipid−graphene structure using the Langmuir−Schaefer (LS) method.[13] We use a variety of structural characterization approaches, namely infrared spectroscopy, ellipsometry, and neutron reflectometry to compare the morphology of a supported lipid bilayer with and without graphene-embedded in the hydrophobic core. We demonstrate that the structure remains stable and graphene does not affect the natural configuration of the lipids within the bilayer assembly, in line with simulation results.

Graphene is encapsulated within the hydrophobic core of a 1,2-distearoyl-*sn*-glycero-3-phosphocholine (DSPC) bilayer using a three-step protocol: (i) First, a DSPC monolayer is transferred on to an oxidized silicon wafer using the Langmuir−Blodgett[27] method: The saturated DSPC lipids are predeposited at the air−water interface of a Langmuir trough and compressed to obtain a stable monolayer with a surface pressure (π) of 40 mN/m. The lipid monolayer is then transferred on to the wafer by retracting the substrate from the trough at a constant π, obtaining a transfer ratio of approximately 1. (ii) Second, graphene is transferred atop the DSPC monolayer: The ordered lipids on the substrate are brought into contact with graphene floating on an ammonium persulfate solution (0.5 M)[28] (the copper foil on which the graphene was initially grown is first etched using ammonium persulfate,[29] see the Supporting Information for experimental details). Eventually, (iii) the second DSPC monolayer is transferred on to the lipid−graphene heterostructure by carefully and controllably lowering the wafer horizontally into contact with a compressed lipid monolayer (π = 40 mN/m). Figure 1 details the fabrication process. After each fabrication step, the structure was characterized systematically using infrared reflection absorption spectroscopy (IRRAS) and ellipsometry. We also precisely studied the hybrid superstructure with angstrom resolution using neutron reflectometry.

Figure 2a illustrates the IRRAS spectra corresponding to the DSPC lipid monolayer (step I, black line), after transferring the graphene atop DSPC (step II, blue line), and after the deposition of the second DSPC monolayer (step III, green line). The absorption bands correspond to the symmetric and asymmetric methylene (CH_2) stretching vibrations of the lipid acyl chains. The peaks are fitted with a Gaussian model. Deposition of the graphene on the lipid monolayer (step II) red shifts the symmetric CH_2 vibration from 2911.0 ± 0.1 to 2909.3 ± 0.1 cm^{-1} and in the asymmetric CH_2 vibration from 2844.1 ± 0.1 to 2842.1 ± 0.1 cm^{-1}. The shift is due to an increase in the trans-conformation within the lipid chains,[30] yielding an overall reordering of the lipids, as we reported earlier.[26] The absorption band intensity, on the other hand,

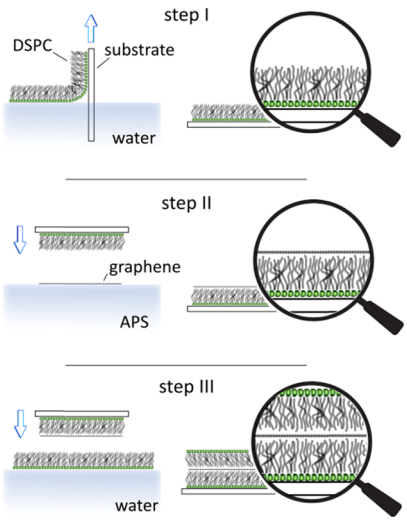

Figure 1. Fabrication of the lipid encapsulated graphene heterostructure. The fabrication protocol is composed of three major steps: Lipids are first transferred on to the already immersed wafer via the Langmuir−Blodgett approach (step I). The hydrophilic head groups are in contact with the oxidized surface of the wafer. Next, graphene, floating on the surface of a copper etching agent, is transferred on to the lipid monolayer by gradually lowering the lipids into contact with graphene (step II). The fabrication is completed by transferring the second lipid layer via the Langmuir−Schaefer approach where the second lipid layer is picked horizontally on to the graphene/lipid assembly (step III).

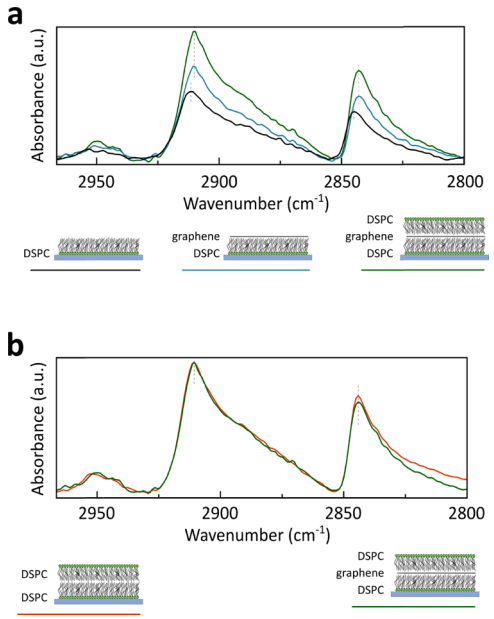

Figure 2. IRRAS spectra of (a) DSPC monolayer deposited on Si/SiO_x substrate (black line); DSPC monolayer with graphene deposited on top (blue line); and DSPC bilayer with the graphene inserted in the hydrocarbon chains (green line). (b) DSPC bilayer (orange line) and DSPC with graphene in the hydrophobic core of the lipid bilayer (green line). All the measurements were performed in air.

increases, which is attributed to an expansion of the lipid chains in a more organized structure.[26] Upon the transfer of a second lipid monolayer atop graphene, the intensity of the absorbance bands increased even further, associated with an

https://dx.doi.org/10.1021/acs.langmuir.0c01691
Langmuir 2020, 36, 14478−14482

increase in the amount of lipids, i.e., the complete transfer of a DSPC monolayer on top of graphene.

To understand how the second lipid monolayer structurally organizes on top of graphene and whether or not graphene destabilizes the two individual DSPC monolayers below and above, a DSPC lipid bilayer on the substrate without graphene was prepared as a control and compared to the DSPC−graphene−DSPC assembly (Figure 2b). The similarity of the IRRAS spectra implies that graphene does not significantly disturb the IRRAS fingerprint of the lipid bilayer, confirming a stable lipid−graphene−lipid structure.

Ellipsometry determines the thickness of the structures at different fabrication steps (Figure 3). The bare DSPC

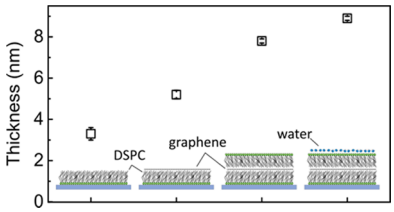

Figure 3. Thickness of different DSPC−graphene heterostructures as measured by ellipsometry.

monolayer measures a thickness of 3.3 ± 0.3 nm, which is in agreement with the neutron reflectometry data (to be discussed later) that provides the thickness of a single DSPC monolayer with the contribution of a layer of water between the substrate and the lipid head groups (see Supporting Information, Table S.1). The deposition of graphene atop increases the thickness to 4.8 ± 0.2 nm. The increment of ∼1.5 ± 0.5 nm in the lipid thickness is in line with our earlier observation,[26] which could partially be attributed to the improved order of the lipid layer. In fact, the hydrophobic interaction between graphene and the lipid tail groups minimizes the random wobbling of the latter; lipids adopt a more compact and well-organized structure, where the compression from the surrounding pushes the tails to largely extend, increasing the layer thickness. We note that the existence of an air gap between the graphene and the tails of the lipids is also likely, which calls for further theoretical/experimental analysis.

Finally, a second DSPC monolayer was transferred atop the graphene−lipid monolayer assembly. This process could naturally result in the presence of a thin water layer at the surface of the assembly due to the hydrophilic nature of the lipid head groups. The data is therefore analyzed with and without assuming the water layer in the constructed model. In the dry state, the thickness obtained for the second DSPC monolayer is 2.6 ± 0.1 nm, whereas, in the wet state, the DSPC monolayer thickness reaches a value of 3.7 ± 0.1 nm, suggesting that the lipid head groups still retained some water in their vicinity, as the obtained value is comparable to the thickness measured for the first DSPC monolayer. Neutron reflectometry data (see below) showed a thickness of 2.6 nm for the second DSPC monolayer transferred on top of graphene, where the sample was kept in a liquid environment all the time. Nevertheless, for the reflectivity data, the water layer on top of the second lipid monolayer transferred is considered as a semi-infinite medium (thickness of a few hundred micrometers).

IRRAS and ellipsometry experiments demonstrated the successful realization of the graphene sandwiched between lipid monolayers. Neutron reflectometry (NR) measurements provide a molecular-scale characterization of the resulting structure; the experiments were performed at the Institut Laue-Langevin, Grenoble (D17 reflectometer, doi: 105291/ILL-DATA.9-13-734 and 105291/ILL-DATA.EASY-341). NR is a nondestructive technique that provides information about the thickness, roughness, hydration, and composition of the lipid layers at a fraction of nanometer in the direction normal to the surface. Similar to ellipsometry, the technique resolves different constituent layers by measuring the corresponding scattering length density (SLD), which depends on the layer composition (see the Supporting Information). The samples were prepared on a 5 × 5 cm^2 single-crystal silicon with a natural oxide layer of 1.1 ± 0.1 nm, estimated by an initial NR characterization (see the Supporting Information). The silicon blocks were cleaned with solvents and plasma prior to the deposition of the structures and measured in three different water contrasts (H_2O, D_2O and silicon-matched water, SMW consisting of 32% D_2O and 68% H_2O). The NR measurements of the DSPC with and without graphene are performed in a solid/liquid cell that allows a continuous contact of the sample with bulk water. Note that the initial visual inspection of the samples with graphene estimated the graphene coverage of 30 ± 10% (see the Supporting Information). The specular reflectivity profiles of the DSPC bilayer with graphene in the gel phase (T = 25 °C) at three different contrasts, H_2O (blue), SMW (green), and D_2O (red) and the corresponding SLD profiles demonstrate that the integrity of the lipid bilayer is preserved in the presence of graphene (Figure 4a,b). The result is in line with the IRRAS measurement (Figure 2b). The measurements made using a 2D detector shows no off-specular component

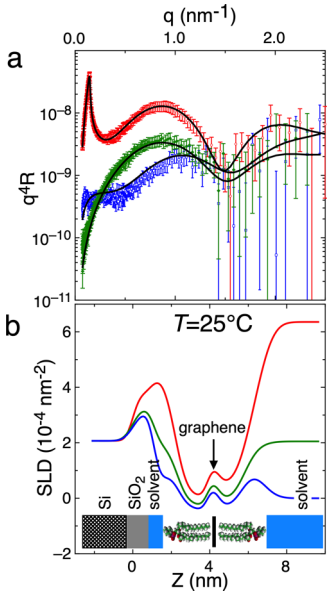

Figure 4. (a) Neutron reflectivity profiles displayed as Rq^4 vs q (where R is the reflectivity and q is the wave vector transfer) from a DSPC bilayer at 25 °C (gel phase) in three contrasts: D_2O (red), silicon-matched water (SMW, green), and H_2O (blue). The solid lines correspond to the best fitting with the model explained in the Materials and Methods section. (b) The corresponding SLD profiles in three contrasts: D_2O (red), SMW (green), and H_2O (blue). Parameters corresponding to the best fits are given in Table S3.

https://dx.doi.org/10.1021/acs.langmuir.0c01691
Langmuir 2020, 36, 14478−14482

(data not shown), even with limited graphene coverage.[31] The graphene monolayer does not significantly alter the reflectivity curve, most likely due to the limited graphene surface coverage, resulting in a SLD value lower than expected (Figure 4b, see Table S1 in the Supporting Information). Therefore, although the analysis of the reflectivity data is consistent with the presence of a graphene sheet between the two lipid layers, it fails to provide robust evidence as the data can be fitted also with a model excluding this layer. The transfer of graphene on top of the lipid monolayer is indeed confirmed by ellipsometry measurements, visual inspection (see Supporting Information, Figure S1), and Raman spectroscopy.[26]

Finally, we studied the stability of the lipid−graphene superstructure when the bilayer was in the fluid phase (T = 55 °C). The results presented in the SI clearly show that the superstructure remains stable with probably a more ordered structure of the outer leaflet of the bilayer compared to the gel phase probably due to the annealing of the sample.

The successful assembly of graphene within the hydrophobic core of a DSPC bilayer is demonstrated and characterized in detail using infrared reflection absorption spectroscopy, ellipsometry, and neutron reflectivity. We observed a stable arrangement of lipid layers both below and above graphene, with no significant graphene-related perturbation compared to a plain lipid bilayer. Our results are in agreement with simulations results. The confirmed possibility of inserting a graphene layer within the hydrophobic core of a lipid bilayer opens up a route for directly probing membrane-related processes in situ using graphene as an electrical sensor. An optimization of the deposition process, leading to an improvement of the graphene coverage rate for large samples could allow more accurate characterization of the graphene layer in the lipid−graphene superstructure.

■ ASSOCIATED CONTENT

Supporting Information

The Supporting Information is available free of charge at https://pubs.acs.org/doi/10.1021/acs.langmuir.0c01691.

Materials and methods; complementary NR experiments; the image of the 5 × 5 cm^2 silicon block showing the graphene transferred on top, with a coverage of 30 ± 10%; neutron reflectivity profiles displayed as Rq4 vs q from a DSPC bilayer at 25 °C (gel phase) and 55 °C (fluid phase); scattering length density (SLD) values used for the fitting procedure; parameters obtained from best fits for DSPC pristine bilayer at 25 °C; parameters obtained from best fits for the DSPC−graphene superstructure at 25 °C; and parameters obtained from best fits for the DSPC−graphene superstructure at 55 °C (PDF)

■ AUTHOR INFORMATION

Corresponding Author

Grégory F. Schneider − *Department of Supramolecular & Biomaterials Chemistry, Leiden Institute of Chemistry, Leiden University, 2300 RA Leiden, The Netherlands;* orcid.org/0000-0001-5018-3309; Email: g.f.schneider@chem.leidenuniv.nl

Authors

Hadi Arjmandi-Tash − *Department of Supramolecular & Biomaterials Chemistry, Leiden Institute of Chemistry, Leiden University, 2300 RA Leiden, The Netherlands;* orcid.org/0000-0002-2800-8659

Lia M. C. Lima − *Department of Supramolecular & Biomaterials Chemistry, Leiden Institute of Chemistry, Leiden University, 2300 RA Leiden, The Netherlands*

Liubov A. Belyaeva − *Department of Supramolecular & Biomaterials Chemistry, Leiden Institute of Chemistry, Leiden University, 2300 RA Leiden, The Netherlands*

Tetiana Mukhina − *Institut Laue-Langevin, 38042 Grenoble, France; Institut Charles Sadron (ICS), UPR22 CNRS, Université de Strasbourg, 67034 Strasbourg, France*

Giovanna Fragneto − *Institut Laue-Langevin, 38042 Grenoble, France*

Alexander Kros − *Department of Supramolecular & Biomaterials Chemistry, Leiden Institute of Chemistry, Leiden University, 2300 RA Leiden, The Netherlands;* orcid.org/0000-0002-3983-3048

Thierry Charitat − *Institut Charles Sadron (ICS), UPR22 CNRS, Université de Strasbourg, 67034 Strasbourg, France;* orcid.org/0000-0003-3167-6495

Complete contact information is available at: https://pubs.acs.org/10.1021/acs.langmuir.0c01691

Author Contributions

‖H.A.-T. and L.M.C.L. contributed equally to this work.

Notes

The authors declare no competing financial interest.

■ ACKNOWLEDGMENTS

This research was gratefully funded by the European Research Council under the European Union's Seventh Framework Programme (FP/2007-2013)/ERC Grant Agreement no. 335879 project acronym 'Biographene' and the Netherlands Organization for Scientific Research (NWO-VIDI 723.013.007). The authors thank the ILL for beamtime and the use of the PSCM facilities for sample preparation.

■ REFERENCES

(1) Arjmandi-Tash, H.; et al. Zero-Depth Interfacial Nanopore Capillaries. *Adv. Mater.* **2018**, *30*, No. 1703602.

(2) Mannoor, M. S.; et al. Graphene-based wireless bacteria detection on tooth enamel. *Nat. Commun.* **2012**, *3*, No. 763.

(3) Azizi, S.; Nouri-Novin, S.; Seyedsharbaty, M. M.; Zarrabi, F. B. Early skin cancer detection sensor based on photonic band gap and graphene load at terahertz regime. *Opt. Quantum Electron.* **2018**, *50*, No. 230.

(4) Ou, L.; et al. Toxicity of graphene-family nanoparticles: a general review of the origins and mechanisms. *Part. Fibre Toxicol.* **2016**, *13*, No. 57.

(5) Lin, J.; Huang, Y.; Huang, P. Graphene-Based Nanomaterials in Bioimaging, In *Biomedical Applications of Functionalized Nanomaterials: Concepts, Development and Clinical Translation*; Elsevier: 2018; 247−287.

(6) Roy, H.; Bhanja, S.; Panigrahy, U. P.; Theendra, V. K. Graphene-Based Nanovehicles for Drug Delivery, In *Characterization and Biology of Nanomaterials for Drug Delivery*; Elsevier: 2019; pp 77−111.

(7) Eeman, M.; Deleu, M. From biological membranes to biomimetic model membranes. *Biotechnol. Agron. Soc. Environ.* **2010**, 719−736.

(8) Puigpelat, E.; Ignés-Mullol, J.; Sagués, F.; Reigada, R. Interaction of Graphene Nanoparticles and Lipid Membranes Displaying Different Liquid Orderings: A Molecular Dynamics Study. *Langmuir* **2019**, *35*, 16661−16668.

(9) Mao, J.; Guo, R.; Yan, L.-T. Simulation and analysis of cellular internalization pathways and membrane perturbation for graphene nanosheets. *Biomaterials* **2014**, *35*, 6069−6077.
(10) Wang, Q. C.; et al. Heterogeneous oxidization of graphene nanosheets damages membrane. *Sci. China Phys., Mech. Astron.* **2019**, *62*, 1−10.
(11) Li, Z.; Zhang, Y.; Ma, J.; Meng, Q.; Fan, J. Modeling Interactions between Liposomes and Hydrophobic Nanosheets. *Small* **2019**, *15*, No. 1804992.
(12) Tu, Y.; et al. Destructive extraction of phospholipids from Escherichia coli membranes by graphene nanosheets. *Nat. Nanotechnol.* **2013**, *8*, 594−601.
(13) Chen, J.; Zhou, G.; Chen, L.; Wang, Y.; Wang, X.; Zeng, S. Interaction of Graphene and its Oxide with Lipid Membrane: A Molecular Dynamics Simulation Study. *J. Phys. Chem. C* **2016**, *120*, 6225−6231.
(14) Akhavan, O.; Ghaderi, E. Toxicity of Graphene and Graphene Oxide Nanowalls Against Bacteria. *ACS Nano* **2010**, *4*, 5731−5736.
(15) Krishnamoorthy, K.; Veerapandian, M.; Zhang, L.-H.; Yun, K.; Kim, S. J. Antibacterial Efficiency of Graphene Nanosheets against Pathogenic Bacteria via Lipid Peroxidation. *J. Phys. Chem. C* **2012**, *116*, 17280−17287.
(16) Zhang, Y.; et al. Nanotoxicity of Boron Nitride Nanosheet to Bacterial Membranes. *Langmuir* **2019**, *35*, 6179−6187.
(17) Wu, R.; et al. Membrane destruction and phospholipid extraction by using two-dimensional MoS2 nanosheets. *Nanoscale* **2018**, *10*, 20162−20170.
(18) Titov, A. V.; Král, P.; Pearson, R. Sandwiched Graphene−Membrane Superstructures. *ACS Nano* **2010**, *4*, 229−234.
(19) Guo, R.; Mao, J.; Yan, L.-T. Computer simulation of cell entry of graphene nanosheet. *Biomaterials* **2013**, *34*, 4296−4301.
(20) Wang, J.; Wei, Y.; Shi, X.; Gao, H. Cellular entry of graphene nanosheets: the role of thickness, oxidation and surface adsorption. *RSC Adv.* **2013**, *3*, 15776.
(21) Moore, T. C.; et al. Influence of Single-Stranded DNA Coatings on the Interaction between Graphene Nanoflakes and Lipid Bilayers. *J. Phys. Chem. B* **2019**, *123*, 7711−7721.
(22) Lenhert, S.; Mirkin, C. A.; Fuchs, H. In situ lipid dip-pen nanolithography under water. *Scanning* **2010**, *32*, 15−23.
(23) Hirtz, M.; Oikonomou, A.; Georgiou, T.; Fuchs, H.; Vijayaraghavan, A. Multiplexed biomimetic lipid membranes on graphene by dip-pen nanolithography. *Nat. Commun.* **2013**, *4*, No. 2591.
(24) Hirtz, M.; Oikonomou, A.; Clark, N.; Kim, Y. J.; Fuchs, H.; Vijayaraghavan, A. Self-limiting multiplexed assembly of lipid membranes on large-area graphene sensor arrays. *Nanoscale* **2016**, *8*, 15147−15151.
(25) Willems, N.; et al. Biomimetic Phospholipid Membrane Organization on Graphene and Graphene Oxide Surfaces: A Molecular Dynamics Simulation Study. *ACS Nano* **2017**, *11*, 1613−1625.
(26) Lima, L. M. C.; Fu, W.; Jiang, L.; Kros, A.; Schneider, G. F. Graphene-stabilized lipid monolayer heterostructures: a novel biomembrane superstructure. *Nanoscale* **2016**, *8*, 18646−18653.
(27) Yu, Z. W.; Jin; Cao, Y. Characterization of the Liquid-Expanded to Liquid-Condensed Phase Transition of Monolayers by Means of Compressibility. *Langmuir* **2002**, *18*, 4530−4531.
(28) Lima, L. M. C.; Arjmandi-Tash, H.; Schneider, G. F. Lateral Non-covalent Clamping of Graphene at the Edges Using a Lipid Scaffold. *ACS Appl. Mater. Interfaces* **2018**, *10*, 11328−11332.
(29) Arjmandi-Tash, H.; Lebedev, N.; van Deursen, P.; Aarts, J.; Schneider, G. F. Hybrid cold and hot-wall chamber for fast synthesis of uniform graphene. *Carbon* **2017**, *118*, 438−442.
(30) Lewis, R. N. A. H.; McElhaney, R. N. Membrane lipid phase transitions and phase organization studied by Fourier transform infrared spectroscopy. *Biochim. Biophys. Acta* **2013**, *1828*, 2347−2358.
(31) Arjmandi-Tash, H.; Jiang, L.; Schneider, G. F. Rupture index: A quantitative measure of sub-micrometer cracks in graphene. *Carbon* **2017**, *118*, 556−560.

https://dx.doi.org/10.1021/acs.langmuir.0c01691
Langmuir 2020, 36, 14478−14482